DOI: https://doi.org/10.14311/TPFM.2025.005

AEROACOUSTIC SIMULATIONS IN THERMALLY NON-HOMOGENEOUS FLUID FLOWS

M. Caggio[1], M. Schmid[1,2], J. Valášek[1,3], Š. Nečasová[1], T. Bodnár[1,3], O. Starynskyi[4]

[1] **Institute of Mathematics of the Academy of Sciences of the Czech Republic, Žitná 25, 11567, Praha 1, Czech Republic.**

[2] **Department of Mechanics, Materials and Machine Parts Faculty of Transport Engineering University of Pardubice Studentská 95, 532 10 Pardubice, Czech Republic.**

[3] **Faculty of Mechanical Engineering, Czech Technical University in Prague, Karlovo Náměstí 13, 121 35 Prague 2, Czech Republic**

[4] **Doosan Bobcat EMEA, U Kodetky 1810, 263 12 Dobříš, Czech Republic**

Abstract

The cooling system, comprising heat exchangers and cooling fans, is essential for maintaining the power performance and acceptable operational conditions of a vehicle. However, running of the cooling fan produces unwanted noise, which often becomes dominant sound produced by the vehicle. To model the noise generated by turbulent flow and heat transfer around cooling fan blades, an appropriate flow model is essential. This study employs the compressible Navier-Stokes equations with an restricted relation between temperature and density for efficient handling of non-homogeneous temperature fields, combined with Delayed Detached Eddy Simulation (DDES) for advanced turbulence modeling. For the aeroacoustic analysis, a hybrid aeroacoustic approach is adopted, utilizing the Acoustic Perturbation Equation (APE) to model acoustic generation and propagation. The main aim of this study is to model the flow and the acoustic problem in the consistent way for the considered simple test case of heated cylinder walls in cross-flow. As most prior investigations focused only on isothermal conditions the model considered in this study presents an important generalization. A part of the problem is to select an efficient numerical software capable to treat temperature non-homogeneities in the flow and the aeroacoustic solver while being prepared for a possible future industrial application. The obtained results for varying thermal conditions show the significant sensitivity of produced sound pressure levels.

Keywords: Turbulent flows, Computational Fluid Dynamics, Computational Aero-Acoustics, heat transfer.

1 Introduction

The engine bay and its cooling system are essential components of any vehicle, including internal combustion engine (ICE) vehicles as well as battery electric vehicles (BEV). The generated heat needs to be transported to cooling pack consisting of heat exchangers and a cooling fan and dissipated to the surrounding air what produces unwanted noise. In many cases the cooling fan is the primary source of vehicle operation noise, see [1], however in all cases the radiated sound needs to meet strict safety standards, see [9].

The described mechanism of sound generated by a turbulent fluid flow around blades of cooling fan and transporting heat requires to consider an appropriate flow model with a suitably chosen turbulent model capable to deal with heat transport and to describe sound generation in a consistent way. In industry applications the further difficulties appear due to complex geometry of the whole cooling pack. Nevertheless here we restrict ourself to set up an appropriate flow and acoustic model within a simple geometry and to choose an efficient numerical solver, which can be used for future design optimization of cooling fan.

The fully compressible Navier-Stokes equations is definitely a suitable model for the purpose of addressing non-homogeneous temperature field, however, their numerical realization in the most general form even for the considered low Mach number regime is very demanding, see [11], and it leads us to search for acceptable simplifications. For the theoretical analysis of such a problem, we refer to [5]. A promising simplification is to neglect direct density dependence on pressure in the ideal gas law.

Moreover, numerical analysis can be found in [4]. Furthermore, the delayed detached eddy simulation (DDES) is here chosen as an advanced turbulence model, [13]. Its advantage is the ability to provide accurate predictions of turbulent flows while remaining computationally efficient. In particular, the RANS model is used in regions near solid boundaries, where fine resolution is essential but computational costs can be prohibitive, and the improved (delayed) transition to the LES model is applied in outer regions, capturing the flow in greater detail. Due to its computational benefits and better ability to capture flow separation, it became an industrial standard; see [12].

The current state-of-the-art computational aeroacoustics (CAA) uses hybrid approaches that separate flow and acoustic descriptions, [12, 10, 15]. Its advantage is to approximate directly the acoustic pressure, which usually has a tiny magnitude compared to the overall pressure involved in the flow dynamics; a possibility to use problem-specific solvers as well as to utilize meshes that meet various requirements. The fluid mesh primarily needs to have well resolved boundary layers where the acoustic mesh can be more sparse but on the other hand the acoustic simulation is usually performed in a larger domain, [10].

The acoustic perturbation equation (APE) is here preferred for the aeroacoustic analysis besides other options like Lighthill's analogy (LH), Ffowcs-Williams and Hawkings' (FWH) formulation or the Kirchhoff method, [10]. It is based on a careful splitting of flow quantities on the acoustic and non-acoustic components and its advantage is the model of acoustic sources in the form of time derivative of incompressible pressure component, see [3], as it requires less storage space and the numerical approximation of time derivative is usually less prone to introduce unwanted numerical noise compared to the LH, [10].

Many studies have explored the aeroacoustics of the cooling fan, some of them including heat exchangers, however these investigations have been conducted almost exclusively under isothermal conditions, see CAA benchmark of axial fan [12] and similar works [18, 15, 1]. Strong connections between heat and flow interactions in the cooling fan and heat exchanger configuration were demonstrated in e.g. [16]. Thus in this paper we will try to address this missing gap and to investigate the influence of the heated cylinders in cross-flow on the produced sound pressure levels.

The paper is organized as follows: The second section provides a mathematical description of the fluid flow and the aeroacoustic problem. The third section presents the details of the numerical setup and acoustic results for three different temperatures of heated cylinder walls. Finally, the conclusion summarizes the obtained results and outlines future perspectives.

2 Mathematical model

In the following, we briefly describe the mathematical model that will be considered in our analysis.

Fluid dynamic model The fluid dynamic model consists of the compressible Navier-Stokes equations describing a heat conducting perfect gas:

$$\partial_t \rho + \nabla \cdot (\rho \boldsymbol{u}) = 0 \quad ; \tag{1}$$

$$\partial_t (\rho \boldsymbol{u}) + \nabla \cdot (\rho \boldsymbol{u} \otimes \boldsymbol{u}) = -\nabla p + \nabla \cdot \tau \quad ; \tag{2}$$

$$\partial_t (\rho \boldsymbol{u} h) + \nabla \cdot (\rho \boldsymbol{u} h) = \partial_t p + \boldsymbol{u} \cdot \nabla p + \tau \cdot \nabla \boldsymbol{u} + \nabla \cdot (\alpha \nabla h) \quad . \tag{3}$$

Here, $\rho = \rho(x,t), p = p(x,t)$ and $\boldsymbol{u} = \boldsymbol{u}(x,t)$ are the density, pressure and the velocity of the fluid, respectively, functions of the space x and time t. The enthalpy $h = c_p T(x,t)$, with T temperature of the fluid, R perfect gas constant, c_p specific heat capacity at constant pressure and α thermal diffusivity, these last two assumed constant due to small changes with the temperature.

From the numerical simulation perspective, being the Mach number low, the density differences are small compared to the background reference density. Consequently, the fluid behavior near the incompressible fluid limit allows decoupling density from pressure dependence. Instead, it only depends on the temperature and the reference pressure, namely

$$\rho = \frac{p_{ref}}{RT}. \tag{4}$$

Further, the quantity τ represents the viscous stress tensor given by the following relation

$$\tau = 2\mu(T)\mathbb{D} - \frac{2}{3}\mu(T)(\nabla \cdot \boldsymbol{u})\mathbb{I} \qquad \text{with} \qquad \mathbb{D} = \frac{1}{2}\left(\nabla \boldsymbol{u} + (\nabla \boldsymbol{u})^T\right)$$

and the dynamic viscosity μ given by the Sutherland's law

$$\frac{\mu(T)}{\mu(T_0)} = \left(\frac{T}{T_0}\right)^{3/2}\left(\frac{T_0 + S}{T + S}\right)$$

where the reference temperature $T_0 = 273K$ and the Sutherland constant $S = 110K$ (see e.g. [6]).

Acoustic model The acoustic model is derived in the framework of the acoustic/viscous splitting approach (see e.g. Kaltenbacher [10] and references therein). The idea is that the flow field quantities are split into averaged and fluctuating part. A suitable model for our purposes comes from the proposal of Ewert and Schröder [3] in which the authors derived an acoustic system based on the following decomposition

$$\boldsymbol{u} = \overline{\boldsymbol{u}} + \boldsymbol{u}^{(ic)} + \boldsymbol{u}^{(a)}, \qquad p = \overline{p} + p', \qquad \rho = \overline{\rho} + \rho' \tag{5}$$

in which the fluctuation contains both the incompressible and compressible part. Here, (ic) stands for incompressible and index (a) for the (irrotational) acoustic component. The pressure fluctuation $p' = c^2\varrho'$ and $p' = p^{(ic)} + p^{(a)}$. The quantity $c = \sqrt{\gamma RT}$ is the speed of sound, function of the temperature, with γ adiabatic constant. The quantity $\overline{\boldsymbol{u}} + \boldsymbol{u}^{(ic)}$ is solenoidal and the overbar means a space-time averaging. The model derived in [3] reads as follows [1]:

$$\partial_t \varrho' + \operatorname{div}(\varrho'\overline{\boldsymbol{u}} + \overline{\varrho}\boldsymbol{u}^{(a)}) = 0, \qquad \partial_t \boldsymbol{u}^{(a)} + \nabla(\overline{\boldsymbol{u}} \cdot \boldsymbol{u}^{(a)}) + \nabla\left(\frac{p^{(a)}}{\overline{\varrho}}\right) = 0,$$

$$\partial_t p^{(a)} - \overline{c}^2 \partial_t \varrho' = -\partial_t p^{(ic)},$$

where $\overline{c} = \sqrt{\gamma R \overline{T}}$ and, for low-Mach number flows, sound sources coming from vortical perturbations, temperature and entropy fluctuations could be neglected. Now, substituting the last equation into the first, we have

$$\frac{1}{\overline{c}^2}\partial_t(p^{(a)} + p^{(ic)}) + \operatorname{div}(\varrho'\overline{\boldsymbol{u}} + \overline{\varrho}\boldsymbol{u}^{(a)}) = 0, \qquad \partial_t \boldsymbol{u}^{(a)} + \nabla(\overline{\boldsymbol{u}} \cdot \overline{\boldsymbol{u}}^{(a)}) + \nabla\left(\frac{p^{(a)}}{\overline{\varrho}}\right) = 0.$$

Due to the fact that the convective velocity has usually a negligible effect in low-Mach number flows, another simplification of the above model consists in assuming $\overline{\boldsymbol{u}} = 0$, obtaining

$$\partial_t(p^{(a)} + p^{(ic)}) + \overline{\varrho}\,\overline{c}^2 \operatorname{div}(\boldsymbol{u}^{(a)}) = 0, \qquad \overline{\varrho}\partial_t \boldsymbol{u}^{(a)} + \nabla p^{(a)} = 0.$$

Now, applying (∂_t) to the first equation and $(\overline{c}^2\nabla\cdot)$ to the second equation and subtract the two resulting equations, we end up with our acoustic model

$$\frac{1}{\overline{c}^2}\partial_{tt} p^{(a)} - \Delta p^{(a)} = -\frac{1}{\overline{c}^2}\partial_{tt} p^{(ic)}. \tag{6}$$

The above equation is usually termed aero-acoustic wave equation (see Kaltenbacher [10]) with $\partial_{tt} p^{(ic)}$ as a source term.

3 Aeroacoustic simulation

The fluid dynamics and aeroacoustic models described in the previous section were applied to a simplified test case designed to illustrate the important role of temperature-dependent air density and viscosity in aeroacoustic results. This test case geometry mimics a heat exchanger, a commonly encountered heat source in cooling systems.

[1] In [3], the continuity and the momentum equations are expressed in terms of the enthalpy and the velocity of the fluid as primary variables with the help of the thermodynamic relation $(\nabla p/\rho) = \nabla h - T\nabla s$, with T and s being temperature and entropy of the fluid, respectively. This formulation, however does not consider an equation for the enthalpy, is consistent with our fluid dynamics model.

Flow setup. The geometry of the test case comprises a box-shaped tunnel with two perpendicular pipes, as shown in Figure 1 with all dimensions and a detailed description of the setup. Heat is introduced into the considered system via Dirichlet boundary conditions applied to the pipe surfaces, prescribing here constant temperatures. Three different thermal conditions are investigated: the pipe surfaces heated to 20°C, 100°C and 500°C. The thermal conductivity of air and the specific heat capacity are prescribed as constant values: $\alpha = 0.025\,\mathrm{W/(m \cdot K)}$ and $c_p = 1005\,\mathrm{J/(kg \cdot K)}$, respectively. The following boundary conditions are considered for this test:

- at the inlet is prescribed velocity of 10 m/s and constant temperature 20°C,
- the tunnel walls are modelled with no-slip Dirichlet boundary condition,
- at the outlet the pressure is fixed at 0 Pa together with a zero-gradient velocity condition.

The Reynolds number defined with the help of the inlet velocity and the reference length equal to the diameter of the pipe is approximately 13,000 and the Mach number is 0.03. These conditions justify the assumption of a negligible average flow velocity $\overline{\boldsymbol{u}}$, whose low magnitude relative to the speed of sound should not significantly impact the propagation of aeroacoustic waves. However, average flow velocity could have an effect, for example, in scenarios involving rotating geometries, such as cooling fans; nevertheless, this study focuses exclusively on the temperature effect, and the effects of average flow velocity are here neglected.

The mathematical model is numerically simulated in the commercial software Siemens Star-CCM+ (v19.06-008). The software employs the so-called *incompressible ideal gas model* to account for temperature-dependent density variations – see Eq. (4) and also [13], accompanied here by a reference pressure of 101,325 Pa. The applied turbulence model is Spalart-Allmaras Improved Delayed Detached Eddy Simulation (SA-IDDES) using a segregated solver, consistent with the methodology outlined in [12], where they achieved good agreement with experimental measurement.

The computational mesh is depicted in Figure 2, consisting of approximately 3.3 million cells. Ten prism layers are included to achieve a maximum $y+$ value of 0.6, ensuring accurate resolution of the viscous boundary layer without relying on wall functions. The base cell size of 2 mm, consistent with [12], is sufficient to resolve the airflow and acoustic fields, given the relatively low vortex shedding frequency compared to typical fan flows.

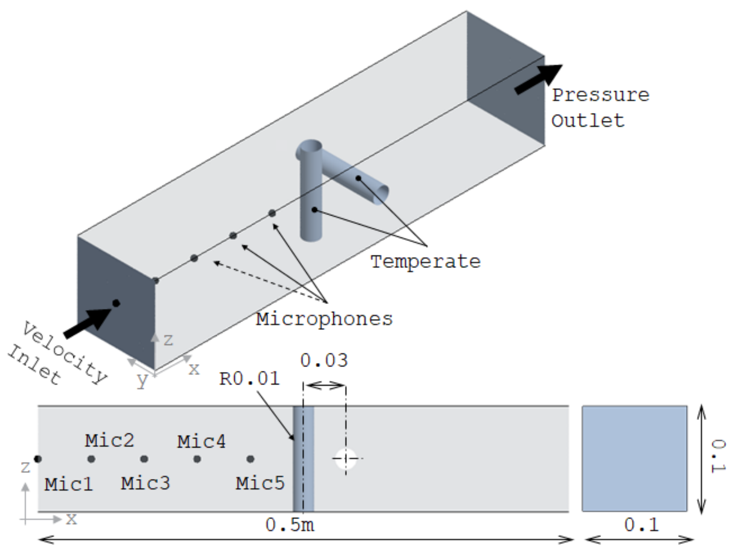

Figure 1: The geometry of the test case domain.

Acoustic setup. The aeroacoustic simulation is based on the model described by equation (6), with fully reflective boundary conditions applied to all tunnel and cylinders walls, while non-reflecting boundary conditions are used at the inlet and outlet [13]. The computational mesh used for aeroacoustics is identical to the one used for the flow simulation as shown in Figure 2.

The speed of sound $\bar{c}$ is calculated with the help of the spatially and temporally averaged temperature $\overline{T}$ as $\bar{c} = \sqrt{\gamma R \overline{T}}$. Here, $\gamma = 1.4$ represents adiabatic index of atmospheric air (diatomic gas) and R denotes the specific gas constant with a value of $R = 287.05 J/(kgK)$. The time step of 10^{-6} s is used and the simulation duration is 1.1 s, where the first 0.1 s of the simulation is excluded from the aeroacoustic analysis. Five virtual probe microphones, numbered 1 to 5 along the x-axis - see Fig. 1, are used to capture time-dependent acoustic pressure.

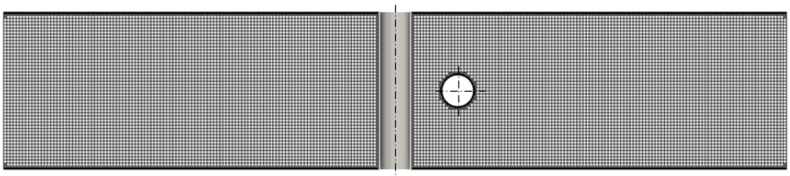

(a) Computational mesh used for fluid flow simulation.

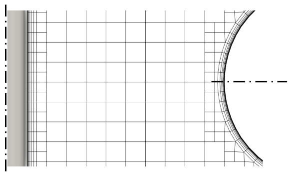

(b) Detail of the mesh in the region between two pipes.

Figure 2: Visualization of the computational mesh: (a) overall mesh and (b) detailed view.

Results of numerical simulation. Results for velocity magnitude and temperature at the final time step are presented in Figure 3, while the density variations along a central line from the inlet to the outlet are shown in Figure 4. These density variations, computed using *the incompressible ideal gas model*, influence airflow and subsequently the characteristics of aeroacoustic sources. Further, the averaged speed of sound does not vary significantly with increasing temperature, see Table 1.

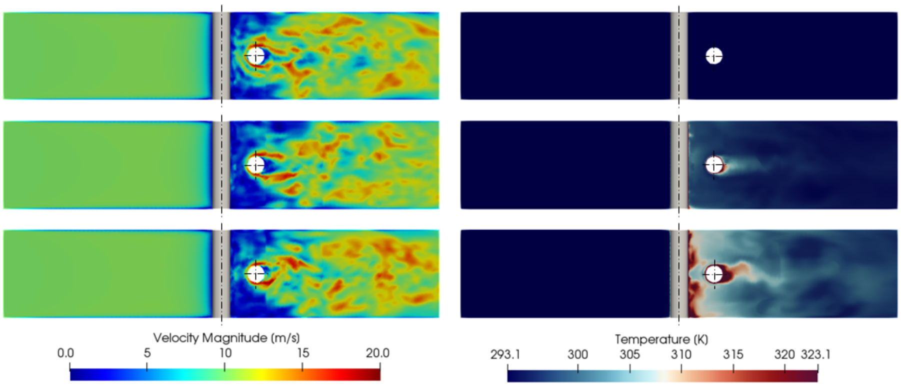

Figure 3: Velocity magnitude (left) and temperature field (right) shown for the cut in plane $y = 0.05$ m at the final time step. The results for $T = 20$°C, 100°C and 500°C are in the top, the middle and the bottom row, respectively.

On the other hand, the impact of temperature on the acoustic pressure documented by sound pressure levels (SPL) at five microphone positions is summarized in Table 1. It demonstrates quite significant SPL variations across different thermal conditions, which could be expected as variation of the density is quite large as shown in the Figure 4. Also recent research [8] has achieved a noise reduction of several dB, while maintaining the same input parameters of the flow field.

The frequency spectra of acoustic pressure monitored at microphone probes and presented as 1/3-octave sound pressure levels are shown in Figure 5. A peak near 160 Hz corresponds to the vortex shedding frequency, which aligns reasonably well with the theoretical frequency for a cylindrical body, calculated using Strouhal number of 0.214, see [2], [7]. Notably, the reduced fluid density due to higher temperatures leads to a decrease in the amplitude of this peak.

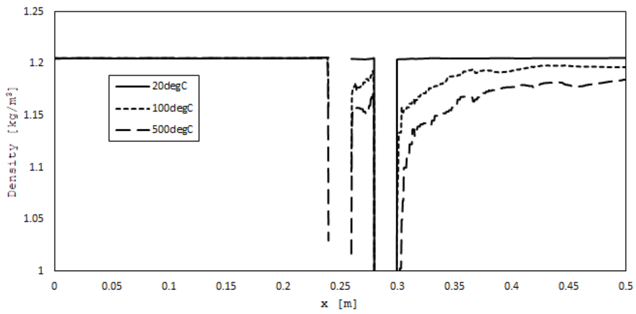

Figure 4: The density variations along the central line $y = z = 0.05\,\mathrm{m}$ for varying thermal conditions. The plot interrupts correspond with the location of pipes.

Overall SPL [dB]			
Microphone	20°C	100°C	500°C
1	127.5	116.7	111.4
2	127.4	116.5	111.2
3	127.0	116.2	110.9
4	126.5	115.6	110.3
5	125.6	114.8	109.5
Averaged speed of sound [m/s]			
$\overline{c}$	343.25	343.51	344.53

Table 1: Overall SPL in [dB] calculated at microphone positions together with calculated averaged speed of sound for different thermal conditions.

4 Conclusions and future perspectives

It can be observed from the data in Table 1 that imposed heat in the system leads to a reduction of the overall sound pressure level (SPL) with increasing temperature. The largest difference is obtained for Microphone 1, where the SPL decreases from 127.5 dB at 20°C to 111.4 dB at 500°C, which corresponds to a reduction of approximately 12.6%. Similarly, the SPL at 100°C for Microphone 1 is 116.7 dB, indicating a reduction of around 8.5% compared to the 20°C condition. In particular, the detailed view at resulting acoustic spectrum shows a clear reduction of the dominant peak at 160 Hz with increasing temperature. The results of the test case highlight the important influence of the temperature field on aeroacoustic sources through temperature-dependent material properties, namely viscosity and density. The influence has the order of magnitude of several decibels, comparable to the levels considered in optimization studies of cooling fans [9] or entire vehicle cooling pack systems [8, 14], thus significant.

However, it is important to note that the test case presented in this paper is a simplified representation, where the vortex shedding frequency plays a dominant role. Therefore, the sensitivity to temperature effects should be further investigated within a complete vehicle system to ensure practical applicability and accuracy. We believe that its variance could be still non-neglibile, especially for vehicle heat exchangers with substantial volumes of heated air (introducing large temperature gradients) and it should be further investigated.

Hence a potential future direction is to incorporate these dependencies into simulations involving real vehicle geometries with a cooling fan, taking into account the heat generated by heat exchangers, as e.g. suggested in the PhD thesis [17]. Additionally, the assumption of a negligible mean flow velocity $\overline{\boldsymbol{u}} = 0$ may no longer be valid when considering the presence of a cooling fan with rotating geometry. This requires further refinement of the model to accurately capture the flow dynamics and acoustic interactions.

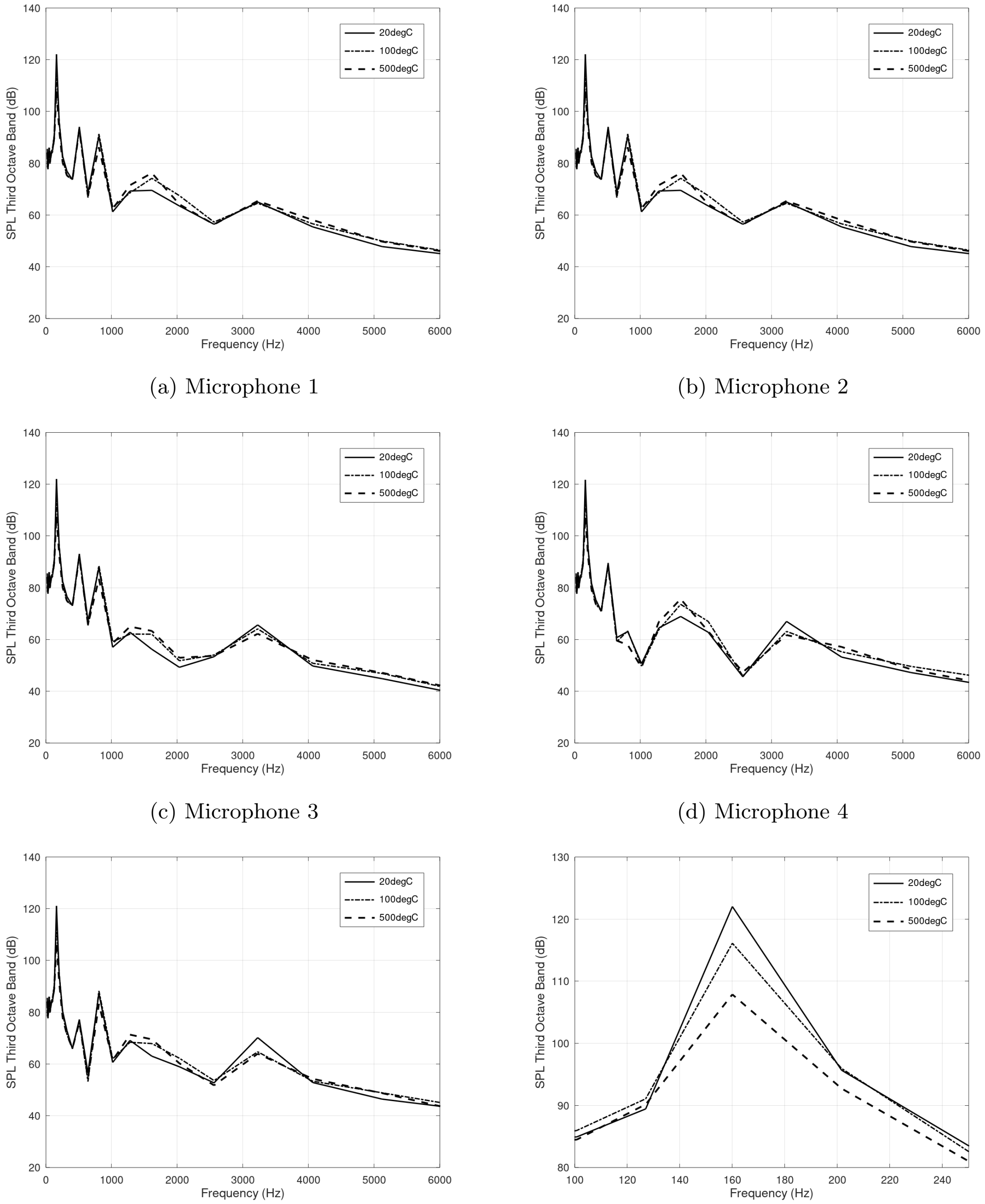

(a) Microphone 1

(b) Microphone 2

(c) Microphone 3

(d) Microphone 4

(e) Microphone 5

(f) Microphone 1 detail

Figure 5: The 1/3-octave frequency spectra of SPL monitored at different microphone probes shown in graphs a)-e). The detail of low-frequency spectrum is presented in the graph f).

Acknowledgment The financial support for the present paper has been provided by the Praemium Academiae of Š. Nečasová. We gratefully acknowledge the support of the Czech Academy of Sciences through RVO:67985840 and Strategy AV21 of the Czech Academy of Sciences within the research programme Breakthrough Technologies for the Future – Sensing, Digitisation, Artificial Intelligence and Quantum Technologies. We would like to also acknowledge the support of Doosan Bobcat EMEA. T. Bodnár, M. Caggio and Š. Nečasová were also supported by the Czech Science Foundation (GAČR) through project GA22-01591S.

References

[1] Allam, S. & Åbom, M.: Noise Reduction for Automotive Radiator Cooling Fans. *Fan2015*, (2015) 17.

[2] Blevins, R. D.: The Effect of Sound on Vortex Shedding from Cylinders. *Journal of Fluid Mechanics*, vol. 161: (1985) pp. 217–237.

[3] Ewert, R. & Schröder, W.: Acoustic perturbation equations based on flow decomposition via source filtering. *Journal of Computational Physics*, vol. 188: (2003) pp. 365–398.

[4] Feireisl, E., Lukáčová-Medvidová, M., Nečasová, Š., Novotný, A. & She, B.: Asymptotic preserving error estimates for numerical solutions of compressible Navier-Stokes equations in the low Mach number regime. *Multiscale Model. Simul.*, vol. 16: (2018) pp. 150–183.

[5] Feireisl, E. & Novotný, A.: Singular limits in thermodynamics of viscous fluids. *Birkhäuser Verlag, Basel*, (2009)

[6] Garnier, E., Adams, N. & Sagaut, P.: Large Eddy Simulation for Compressible Flows. *Springer Science+Business Media B.V.*, (2009).

[7] Guilmineau, E. & Queutey, P.: A Numerical Simulation of Vortex Shedding from an Oscillating Circular Cylinder. *Journal of Fluids and Structures*, vol. 16, no. 6: (2002) pp. 773–794.

[8] Hu, D., Dong, W., Gao, P., Lu, D., Shen, Y., Li, J., Yang, Q. & Wang, J.: Noise reduction optimization for numerous radiator fans for fuel cell vehicles considering thermal-fluid-acoustic synergy. *International Journal of Heat and Mass Transfer*, vol. 223: (2024) pp. 125231.

[9] Kim, J.-H., Ovgor, B., Cha, K.-H., Kim, J.-H., Lee, S. & Kim, K.-Y.: Optimization of the Aerodynamic and Aeroacoustic Performance of an Axial-Flow Fan. *AIAA Journal*, vol. 52, no. 9: (2014) pp. 2032–2044.

[10] Kaltenbacher, M., Marburg, S., Beck, A., Munz, C.-D., Langer, U. & Neumüller, M.: Computational Acoustics. *Springer*, (2018).

[11] Munz, C.-D., Dumbser, M. & Roller, S.: Linearized acoustic perturbation equations for low Mach number flow with variable density and temperature. *Journal of Computational Physics*, vol. 224, no. 1: (2007) pp. 352–364.

[12] Schoder, S., Czwielong, F. & Kaltenbacher, M.: Computational aeroacoustics of the EAA benchmark case of an axial fan. *Acta Acustica*, vol. 4, no. 5: (2020) pp. 22.

[13] Simcenter STAR-CCM+ Version 2410 Documentation. *Siemens Digital Industries Software*, (2024).

[14] Saha, R., Singh, J., Koutsavidis, E. & Ghazialam, H.: Alternate Approach: Acoustics and Cooling Performance Management. *SAE Technical Paper*, no. 2018-01-0084: (2018) pp. 1–9.

[15] Tian, J., Ouyang, H. & Wu, Y.: Experimental and numerical study on aerodynamic noise of outdoor unit of room air conditioner with different grilles. *International Journal of Refrigeration*, vol. 32: (2009) pp. 1112–1122.

[16] Wang, Z., Liu, J., Wang, H., Zhang, B., Liu, W., Özdemir, E. D. & Aksel, M. H.: Numerical and experimental investigation on the integrate performance of axial flow cooling fan and heat exchanger. *Applied Thermal Engineering*, vol. 245: (2024) pp. 609-619.

[17] Zarri, A.: Aerodynamic and Acoustic Investigation of Automotive Fan-Driven Cooling Systems. *PhD Thesis, Université de Lyon & Institut von Karman de dynamique des fluides*, (2021).

[18] Zenger, F., Junger, C., Kaltenbacher, M. & Becker, S.: A Benchmark Case for Aerodynamics and Aeroacoustics of a Low Pressure Axial Fan. *SAE Technical Paper*, no. 2016-01-1805: (2016).